

# Kirkpatrick–Baez mirrors to focus hard X-rays in two dimensions as fabricated, tested and installed at the Advanced Photon Source

Naresh Kujala,\* Shashidhara Marathe, Deming Shu, Bing Shi, Jun Qian, Evan Maxey, Lydia Finney, Albert Macrander and Lahsen Assoufid

Advanced Photon Source, Argonne National Laboratory, 9700 South Cass Avenue, Lemont, IL 60439, USA. \*E-mail: kujala@aps.anl.gov

The micro-focusing performance for hard X-rays of a fixed-geometry elliptical Kirkpatrick–Baez (K–B) mirrors assembly fabricated, tested and finally implemented at the micro-probe beamline 8-BM of the Advanced Photon Source is reported. Testing of the K–B mirror system was performed at the optics and detector test beamline 1-BM. K–B mirrors of length 80 mm and 60 mm were fabricated by profile coating with Pt metal to produce focal lengths of 250 mm and 155 mm for 3 mrad incident angle. For the critical angle of Pt, a broad bandwidth of energies up to 20 keV applies. The classical K–B sequential mirror geometry was used, and mirrors were mounted on micro-translation stages. The beam intensity profiles were measured by differentiating the curves of intensity data measured using a wire-scanning method. A beam size of 1.3  $\mu\text{m}$  (V) and 1.2  $\mu\text{m}$  (H) was measured with monochromatic X-rays of 18 keV at 1-BM. After installation at 8-BM the measured focus met the design requirements. In this paper the fabrication and metrology of the K–B mirrors are reported, as well as the focusing performances of the full mirrors-plus-mount set-up at both beamlines.

**Keywords:** hard X-ray micro-focusing optics; fixed elliptical geometry K–B mirrors; optics and detector beamline.

© 2014 International Union of Crystallography

## 1. Introduction

Third-generation synchrotron facilities are ideal for generating hard X-ray micro-beams because of their very small source sizes and sufficient incident X-ray flux. The focused hard X-rays are useful in the fields of biological samples, nanophase materials, crystal structures, X-ray diffraction and spectroscopy for investigating the structure, elemental distribution and chemical bonding (Ice *et al.*, 2011; Kujala *et al.*, 2011; Larson *et al.*, 2002; Larson & Levine, 2013). The focused micro-beam can be used for the measurement of the trace elemental content of tissue sections directly using X-ray fluorescence, to improve understanding of trace metals and their essential role in health and disease (Paunesku *et al.*, 2012; Weekley *et al.*, 2013).

For more than a decade, various techniques have been developed to produce small focused hard X-ray beams by synchrotron radiation facilities around the world. Smaller spot sizes can be achieved by utilizing different techniques like specular reflection, refraction and diffraction. The techniques so far used at various third-generation synchrotron radiation facilities have incorporated: Kirkpatrick–Baez (K–B) mirrors

(Ice *et al.*, 2000; Yamamura *et al.*, 2003), tapered capillaries (Bilderback, 2003), compound refractive lenses (Snigirev *et al.*, 1996), Fresnel zone plates (Yun *et al.*, 1999), multilayer Laue lenses (Kang *et al.*, 2006), multilayer mirror optics (Mimura *et al.*, 2010) and Bragg–Fresnel optics (Yasa *et al.*, 2004). Among the different types of focusing devices, a reflective optics is useful because various optical designs can be developed over a wide range of X-ray beam acceptances and focal distances. K–B mirrors that utilize total external reflection are known to have the advantage of achromaticity and high efficiency; however, the spot size is ultimately limited by the critical angle (Suzuki, 2004).

A K–B mirrors system can be arranged in two different ways: sequential K–B optics (Kirkpatrick & Baez, 1948; Liu *et al.*, 2005; Ice *et al.*, 2011) and nested, also known as Montel, K–B optics (Montel, 1957; Liu *et al.*, 2011). For sequential K–B optics, X-rays are focused by two sequential elliptical mirrors. For nested K–B optics, the two elliptical mirrors are positioned side-by-side and perpendicular to each other.

A K–B mirrors system consists of two elliptical mirrors each having the X-ray source at a common elliptical focus. One mirror is used for vertical focusing and the other mirror is used

**Table 1**

Root-mean-square residuals and slope errors from best-fit ellipses for 1-BM and 8-BM.

Mirrors	1-BM			8-BM		
	Residual profile (nm)	Residual profile peak–valley (nm)	Slope error ( $\mu$ rad)	Residual profile (nm)	Residual profile peak–valley (nm)	Slope error ( $\mu$ rad)
Vertical focusing mirror	0.61	4.35	0.49	0.67	4.44	0.22
Horizontal focusing mirror	0.35	3.12	0.29	0.31	2.10	0.24

for horizontal focusing. It was entirely designed, developed and tested by the APS optics group and then installed at the 8-BM beamline. The vertical focusing mirror (M1) is 80 mm in length and the horizontal focusing mirror (M2) is 60 mm in length. The focusing performance of an X-ray beam was tested with monochromatic X-rays of 18 keV. In this paper we report on the fabrication and metrology results, mirror mounting stages, testing of elliptical K–B mirrors at the optics and detector test beamline of the APS, namely beamline 1-BM, and the measured performance at the destination beamline 8-BM, a beamline that accommodates fluorescence microprobe users.

The designed ellipse parameters were chosen according to the needs of 8-BM, *i.e.* the distance from the source and distance to the focus, and these were different from those at 1-BM. That is, a different design ellipse would have been chosen for optimum performance at 1-BM. However, the differences in the design ellipses are slight, as shown in Table 1. This is because the design ellipse is insensitive to the distance from the source, and depends primarily on the numerical aperture of the mirror focus. These differences are small enough that test results at 1-BM could be expected to produce an equivalently small focus, albeit at slightly different incident angles on the mirrors. This was so, as borne out in the measured data for the focus. This conclusion is important with regard to being able to use a test beamline with a different source and focal distance than an intended beamline for focus sizes similar to those measured presently, *i.e.* roughly 1  $\mu$ m. We consider this to be a significant novel aspect of the present work.

## 2. Fabrication and metrology

The profile-coating technique developed at the APS (Liu *et al.*, 2012) was used to convert flat Si substrates into precise elliptical mirror surfaces at the APS deposition laboratory. The technique utilizes a contoured mask in a DC magnetron sputtering system with linear motion to coat a predetermined profile onto mirror substrates. The shape of the contour is calculated according to the desired elliptical profile of an ideal final mirror and from the measured shape of the original substrate surface. Very precise elliptical K–B mirrors with sub-nanometer r.m.s heights errors have been obtained (Liu *et al.*, 2004, 2012; Shi *et al.*, 2010). Two flat mirror Si substrates with dimensions of 80 mm (L)  $\times$  20 mm (W)  $\times$  20 mm (H) and 60 mm (L)  $\times$  20 mm (W)  $\times$  20 mm (H) were chosen for sequential K–B optics. Platinum was sputtered to profile coat on the flat Si substrate to make fixed elliptical-shaped mirrors.

Surface profile measurements were obtained at the APS metrology laboratory. A high-resolution non-contact 3D surface profiler was used for the surface figure measurements of the two mirrors. The surface profiler is a microscope designed to measure micro-roughness (model MicroXAM RTS) with five interchangeable objective lenses that can be used to cover a wide range of magnifications from 50 $\times$  with field of view (FOV) 0.24 mm and 0.24 mm, up to 2.5 $\times$  with FOV 4.88 mm and 4.88 mm. Each mirror was tested individually on a high-resolution closed-loop translation stage that was capable of scanning 100 mm in both  $x$  and  $y$  directions to acquire measurement maps at predetermined surface locations. The surface profile of the profile-coated mirror was obtained by stitching together multiple overlapped sub-aperture measurements (Assoufid *et al.*, 2007, 2012; Qian *et al.*, 2012). The size of the measured surface over which figures were measured was 76.78 mm for the vertical mirror and 55.40 mm for the horizontal mirror. The deviations of the measured surface from the best-fit ellipse, often referred to as the residual height error, was 0.67 nm r.m.s for the vertical focusing mirror and 0.31 nm for the horizontal mirror for placement at 8-BM. These values indicate the degree to which the designed ellipse was achieved. The same mirrors when referenced to a different best-fit ellipse calculated for placement at 1-BM had residual errors of only 0.61 nm r.m.s for the vertical focusing mirror and 0.35 nm for the horizontal focusing mirror. That the residual errors are so close is a significant aspect of the present work since they demonstrate the value of carrying out tests at a test beamline. Table 1 shows the parameters for the best-fit ellipse results for micro-stitched interferometry surface height data for the vertical and horizontal focusing mirror, r.m.s deviation from a best-fit ellipse, r.m.s peak-to-valley and r.m.s slope error of the surface profiles for placement at 1-BM and at 8-BM. We can specify the elliptical profile of the mirrors along the reflecting surface using three parameters: source-to-mirror distance, mirror-to-focus distance and the grazing-incidence angle of the X-rays on the mirror source. Table 2 shows the designed parameters of the K–B mirrors for beamlines 1-BM and 8-BM. For 1-BM the source-to-mirror distance for the vertical and horizontal focusing mirrors is 34 m and 34.095 m; mirror-to-focus is 0.250 m and 0.155 m; and grazing-incidence angle is 3.03 mrad and 3.06 mrad, respectively. For 8-BM the secondary source-to-mirror distance for the vertical and horizontal focusing mirrors is 5.75 m and 5.845 m; mirror-to-focus is 0.241 m and 0.152 m; and grazing-incidence angle is 2.82 mrad and 2.93 mrad, respectively.

**Table 2**  
Parameters of the K–B mirrors at beamlines 1-BM and 8-BM of the APS.

Mirrors	1-BM				8-BM			
	Source distance (m)	Focal length (m)	Incident angle (mrad)	Demagnified source size ( $\mu\text{m}$ )	Source distance (m)†	Focal length (m)	Incident angle (mrad)	Demagnified source size ( $\mu\text{m}$ )
Vertical focusing mirror	34	0.250	3.03	0.8	5.75	0.241	2.82	0.51
Horizontal focusing mirror	34.095	0.155	3.06	1.18	5.845	0.152	2.93	0.75

† Secondary source-to-mirror distance of 8-BM.

### 3. Design of the K–B mirrors mounting system

The K–B mirrors mounting stage systems were designed and assembled at the APS. As shown in Figs. 1(a) and 1(b), the APS Y9-64 K–B mirror system consists of two similar sets of mirror mount modules: one mount is for the horizontal reflecting mirror, and the other mount is for the vertical reflecting mirror. The mirror assembly was enclosed in a Plexiglas enclosure mounted on the base plate to provide a helium gas environment for the pair of mirrors. Driven by a pair of PI™ M-110 stepping-motor linear stages, each of

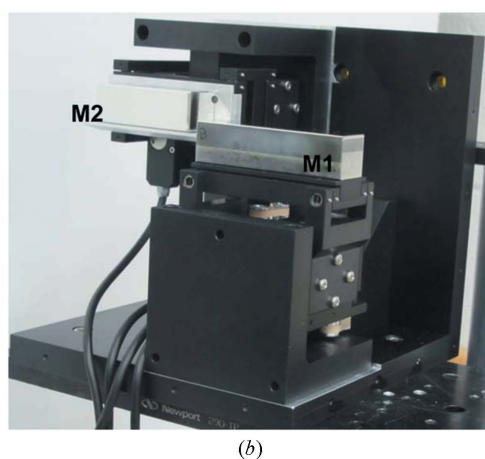
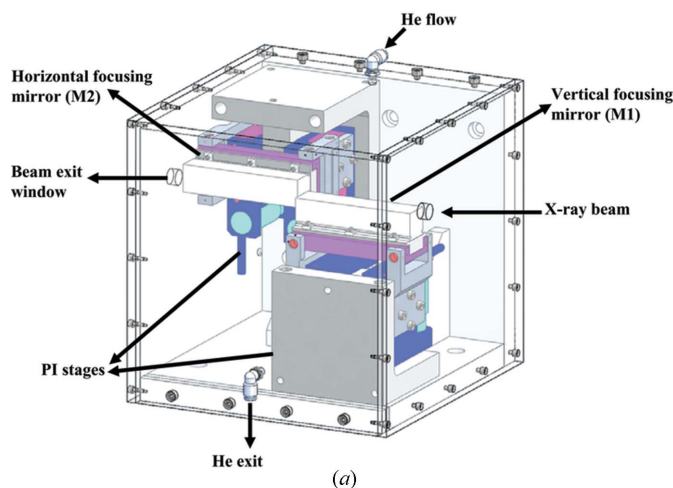


**Figure 1**  
K–B mirror mounting stages: (a) 3D drawing of the Y9-64 mirror mounting stages developed at APS; (b) photograph of the Y9-64 mounting stage with elliptical vertical (M1) and horizontal (M2) K–B mirrors mounted without Plexiglas box.

**Table 3**  
Design specifications of the Y9-64 K–B mirrors mounting stages.

Mirrors mounting stages	80 (L) × 20 (W) × 20 (H) mm
Motor driving stages	M-110.12S
Minimum incremental angular motion	2 $\mu\text{rad}$
Unidirectional angular repeatability	4 $\mu\text{rad}$
Maximum angular travel range	$\pm 2.5^\circ$
Maximum linear travel range	5 mm
Minimum incremental linear motion	0.05 $\mu\text{m}$
Unidirectional linear repeatability	0.1 $\mu\text{m}$
Overall dimensions	169 (L) × 211 (W) × 178 (H) mm

the flexure-pivots-based mechanical modules manipulates a mirror in two dimensions: (i) a linear motion, perpendicular to the mirror optical surface, with 0.1  $\mu\text{m}$  unidirectional repeatability over a 5 mm travel range; and (ii) a mirror pitch angular adjustment with 4  $\mu\text{rad}$  unidirectional repeatability over a maximum  $5^\circ$  travel range. Fig. 1(a) shows a 3D model drawing of the Y9-64 mirror mount stages, and Fig. 1(b) shows the Y9-64 mounting stage with vertical focusing mirror (M1) and horizontal focusing mirror (M2) without the Plexiglas box cover. The mirror mount module Y9-64 is a stepping-motor-driven flexural mechanism with commercial flexural pivots. The flexural bearing structure is operated by two PI™ M-110 motorized linear stages which are mounted on an aluminium module base frame. Operated with the six flexural bearing structures, the M-110 linear stages provide linear positioning in the direction perpendicular to the mirror optical surface, and tilting motion for the mirror pitch adjustment. Table 3 lists the designed specifications of the Y9-64 K–B mirror mounting stages. The opto-mechanical design of the modular X-ray K–B mirror mount system as well as the test results of its precision positioning performance can be found in the paper by Shu *et al.* (2013).

### 4. Experimental set-up

The testing of the K–B mirror system was performed at the Optics and Detector Test Beamline at the Advanced Photon Source, beamline 1-BM. This bending-magnet beamline has been newly reconfigured for optics and detector testing. The beamline consists of three stations A, B and C with only the latter two used for experiments (Lang *et al.*, 1999; Macrander *et al.*, 2013). The Si (111) double-crystal monochromator (DCM) is at 27.5 m from the source. The DCM first crystal is indirectly bottom-cooled by placing it in contact with a water-cooled copper manifold using a Cu–In–Ga eutectic. The monochromator can be tuned over a wide energy range of 6–

**Table 4**

Basic parameters of the K–B mirrors optics system and optical parameters measured at 1-BM.

Mirrors	Length (mm)	Focal length (mm) <sup>†</sup>	Glancing angle (mrad) <sup>†</sup>	Beam acceptance ( $\mu\text{m}$ )	Surface coating material	Demagnification (1-BM/8-BM)	Depth of focus ( $\mu\text{m}$ ) <sup>‡</sup>
Vertical focusing mirror	80	252	2.97	240	Pt	136/214.6	150
Horizontal focusing mirror	60	157	2.97	180	Pt	220/349	100

<sup>†</sup> Measured values during experiments. <sup>‡</sup> Calculated value.

28 keV. The white-beam horizontal and vertical slit openings are 1 mm  $\times$  1 mm. The FWHM of the vertical and horizontal source size of the bending magnet of APS is 110  $\mu\text{m}$  and 260  $\mu\text{m}$ , respectively. The K–B assembly was placed in experimental station B at 34 m from the source. The 80 mm-long elliptical mirror was used for focusing in the vertical plane and the 60 mm-long elliptical mirror was used for focusing in the horizontal plane. This placement of the mirrors corresponded to a geometrical demagnification in the horizontal and vertical equal to 220 and 136, respectively.

The configuration of the K–B mirrors system at 1-BM is shown in Fig. 2. The optical parameters of the mirrors as well as the demagnifications and depth of focus applicable at both beamlines 1-BM and 8-BM are shown in Table 4. The mirror (M1) of length 80 mm was placed upstream and was designed with a focal length of 250 mm for vertical focusing. The mirror (M2) of length 60 mm was placed downstream and was designed to have a focal length of 155 mm for horizontal focusing. The distance between the center of the two mirrors was 95 mm. An incident aperture (set with slits) of 180  $\mu\text{m}$  (V) and 180  $\mu\text{m}$  (H) was located upstream of the K–B mirrors system. The vertical focusing mirror has a horizontal beam acceptance of 240  $\mu\text{m}$ ; however, we limited it to 180  $\mu\text{m}$ . This avoided the edges of the vertical focusing mirror to prevent any possible distortion in the beam profile. The working distance was 110 mm from the downstream edge of the mirror box, which is sufficient for various applications such as scanning X-ray microscopy.

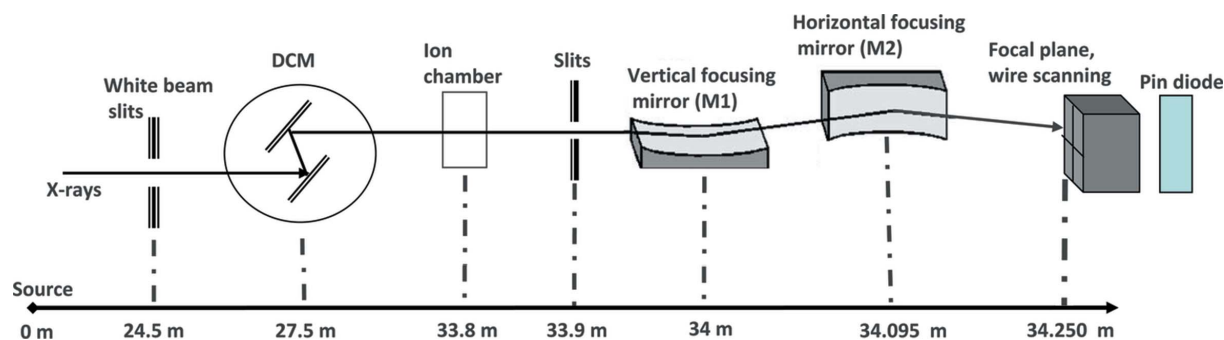
The surface figures of both mirrors were designed to be effective for X-rays with energies below 20 keV. Helium gas was continuously flowed through the Plexiglas enclosure to avoid any radiation damage to the mirrors. The mirror box was mounted on an L-shaped jack, which was mounted on an

optical table. Focusing tests were performed at an X-ray energy of 18 keV. The wire scanning method was used to measure the focused beam size. A tungsten wire was positioned on the XY nano-stage (Physik Instrumente stages) which had a sub-nanometer resolution. The nano-stage was mounted on XYZ translation stages (Kohzu motors) which had a resolution of 1  $\mu\text{m}$  in each Cartesian direction.

Fig. 3 shows the 8-BM experimental layout and configuration of the K–B mirrors system. The beamline has two types of monochromators, which include a double-crystal monochromator (DCM) and double-multilayer monochromator (DMM). For testing the focus performance of the K–B mirrors system the DMM was used at a monochromatic energy of 10 keV and focusing testing was performed using a Cr knife-edge fluorescence scan method. The toroidal mirror is located 31 m from the source, which focused the X-ray beam onto a 150  $\mu\text{m}$  pinhole placed at 17.1 m to produce an effective secondary source distance of 5.75 m and 5.84 m for the vertical and horizontal mirrors, respectively.

## 5. Characterizing the K–B mirrors focusing

Two primary techniques may be used to evaluate the focal spot size of the focused X-ray beam. They are: wire absorption scans and knife-edge fluorescence scans. To measure the nano/micro-focused X-ray beam, the derivative nature of wire-scanning or knife-edge scanning requires high linearity of the translation mechanism. For our studies at 1-BM, the beam profile was measured by scanning a tungsten wire having a diameter of 50  $\mu\text{m}$  and employing a solid-state p-i-n diode as a detector for measuring intensity. The perpendicularity of the two mirrors and the in-surface-plane rotations were adjusted by laser alignment and two X-ray burns made on the entrance

**Figure 2**

Layout of the 1-BM-B station and experimental set-up for the K–B mirrors focusing optics. The geometrical positions of the vertical focusing mirror (M1) of length 80 mm and horizontal focusing mirror (M2) of length 60 mm are shown. The monochromator has a Si (111) double-crystal water-cooled monochromator. The horizontal and vertical slit openings for the slits at 33.9 m were 180  $\mu\text{m}$  (V)  $\times$  180  $\mu\text{m}$  (H). The FWHM of the vertical and horizontal source size of beamline 1-BM is 110  $\mu\text{m}$  and 260  $\mu\text{m}$ , respectively.

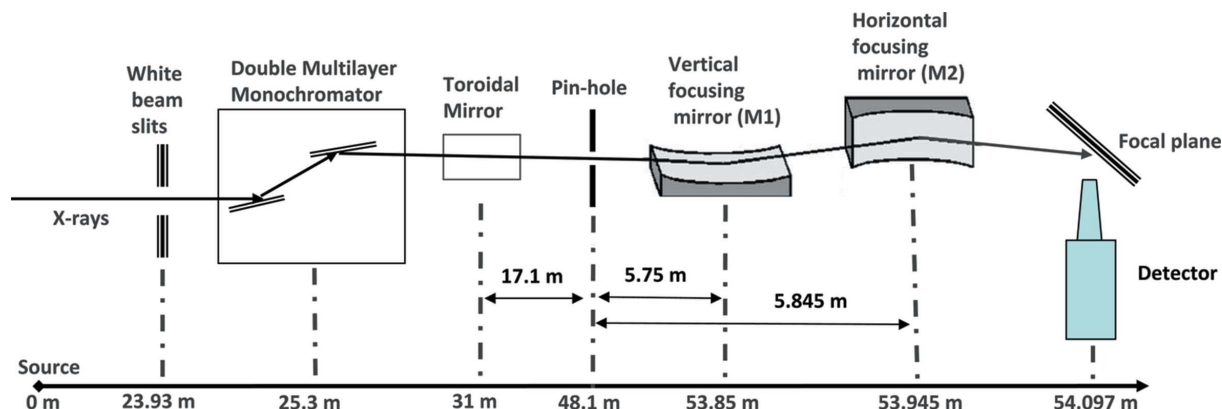


**Figure 3** Layout of the 8-BM station and experimental set-up for the K–B mirrors focusing optics. The geometrical positions of the vertical focusing mirror (M1) of length 80 mm and horizontal focusing mirror (M2) of length 60 mm are shown. The pin-hole of 150  $\mu\text{m}$  diameter is placed at the secondary source.

and exit windows of the K–B mirrors box. After adjusting the glancing angle, the two-dimensionally focused beam profile at 1-BM was measured and is shown in Figs. 4(a) and 4(b). The slits were used to locate the X-ray beam footprints on the mirrors, which were then reflected from the mirrors and focused onto the position where the tungsten wire was supported by an XYZ scanning (Kohzu motors) stage with micrometre resolution.

To locate the focal position along the beam direction at 1-BM we employed a Coolsnap HQ2 CCD detector and an optical system which forms an image by conversion of the X-rays to visible light. We used a scintillator (LYSO) and a 10 $\times$  objective lens combination for image conversion. The scintillator was placed at the common focal plane of two mirrors. This visual method allowed us to tweak the inter-mirror angle to obtain a best focus. For quantitative measurements of the focal spot we subsequently used the wire scanning method.

As shown in Figs. 4(a) and 4(b), we measured a best focus of 1.3  $\mu\text{m}$  (V)  $\times$  1.2  $\mu\text{m}$  (H) with an angle of 2.97 mrad at 1-BM. This was achieved after careful alignment. The tungsten wire was scanned across the beam in both the horizontal and the vertical directions to find the best focus by adjusting both the focal plane distance and the mirror angle. The focused beam intensity profiles were obtained by differentiating the curves of the intensity data collected by the p-i-n diode. The efficiency of the mirrors was 80% at monochromatic energy 18 keV. The best focus was obtained by adjusting the mirror angles and by scanning along the beam propagation.

After validation at 1-BM as discussed above, the entire mirror assembly was delivered to beamline 8-BM as intended. The staff of this beamline made tests to ascertain that the mirrors performed to their intended focus specifications, which were relaxed from those measured at 1-BM. As shown in Figs. 5(a) and 5(b), a measured focused beam size of 1.8  $\mu\text{m}$  (V)  $\times$  2.2  $\mu\text{m}$  (H) with an angle of 2.8 mrad was achieved at 8-BM. The efficiency of the K–B mirror arrangement was found to be 85% at 10 keV. A Cr knife-edge was scanned through the focus in both the horizontal and the vertical directions. Both the measured fluorescence signal intensities as well the derivatives are shown in Fig. 5. Both the focal plane

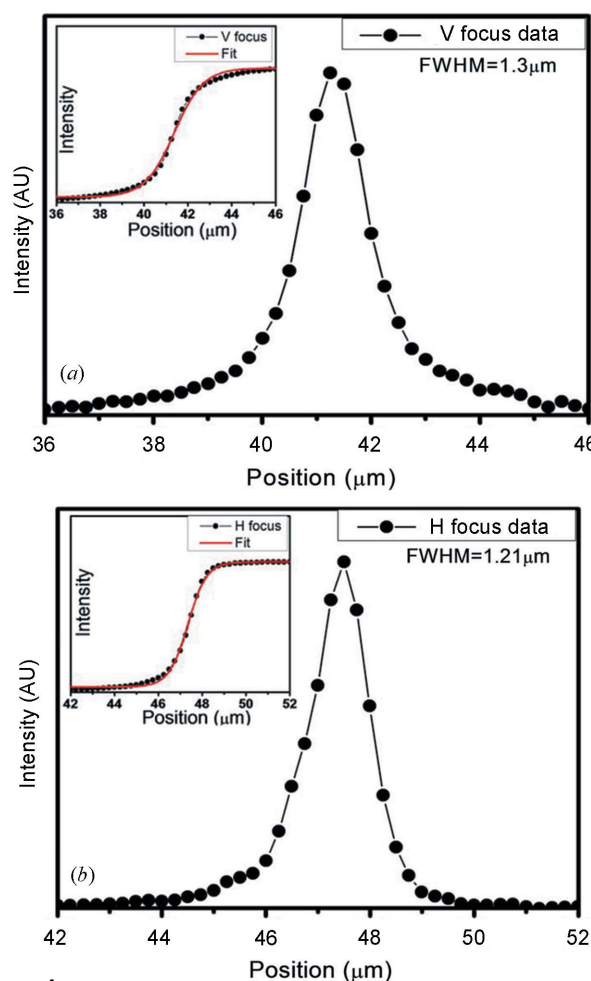


**Figure 4** Profiles of the vertical and horizontal focus measurements of doubly focused spots with a 18 keV monochromatic X-ray beam at beamline 1-BM using tungsten wire absorption scans. (a) Vertical focused beam profile; (b) horizontal focused beam profile. The size of the focus was 1.3  $\mu\text{m}$  (V) and 1.2  $\mu\text{m}$  (H). The inserts in (a) and (b) are the intensity of the tungsten wire scan in the vertical and horizontal directions, respectively.

distance and the mirror angle were adjusted to obtain the results shown. Once the results obtained satisfied the beamline needs, optimization was halted. We do not attribute the



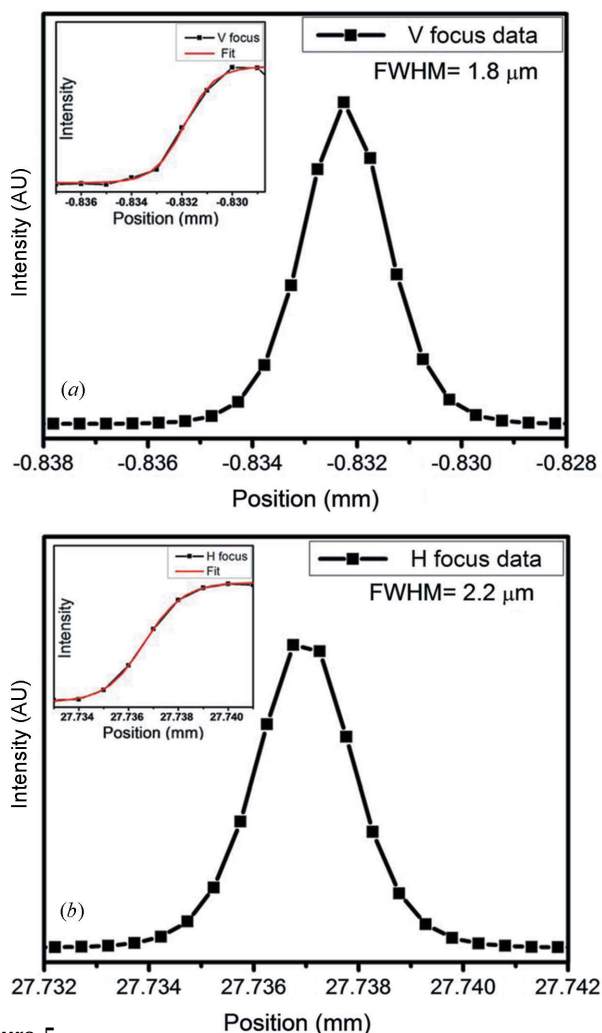


**Figure 5** Profiles of the vertical and horizontal focus measurements of doubly focused spots with a 10 keV monochromatic X-ray beam at beamline 8-BM using Cr knife-edge fluorescence scans. (a) Vertical focused beam profile; (b) horizontal focused beam profile. The size of the focus was  $1.8\ \mu\text{m}$  (V) and  $2.2\ \mu\text{m}$  (H). The inserts in (a) and (b) are the intensity of the scans in the vertical and horizontal directions, respectively.

difference between the results obtained at 1-BM and 8-BM to differences in the beamline layouts, but rather to a better and more determined optimization obtained at 1-BM.

## 6. Conclusions

A complete K–B mirror assembly employing two profile-coated elliptical mirrors was designed and developed by the APS optics group, tested at beamline 1-BM and installed at beamline 8-BM at the Advanced Photon Source. The best possible focus for ideal mirrors that could have been obtained at 1-BM was calculated to be  $0.80\ \mu\text{m}$  for the vertical mirror and  $1.18\ \mu\text{m}$  for the horizontal mirror; for 8-BM these were calculated to be  $0.51\ \mu\text{m}$  for the vertical mirror and  $0.75\ \mu\text{m}$  for the horizontal mirror. These values resulted from the source sizes of the bending-magnet radiation and the demagnifications of the optical set-ups. Here we note that the diffraction limit from a point source for the applicable

numerical apertures is  $\sim 0.2\ \mu\text{m}$ , as calculated from the Rayleigh criterion and verified by wave-optics simulations code (Kewish *et al.*, 2007), so that the ideal resolutions for the present measurements were determined almost entirely by the demagnifications of the optical arrangement. The values at 1-BM should be compared with the measured values at 1-BM of  $1.3\ \mu\text{m}$  vertically by  $1.2\ \mu\text{m}$  horizontally. These values were smaller than were required at 8-BM, and the delivered K–B mirror system was subsequently installed at 8-BM. Tests at 8-BM were performed which ascertained that the mirrors performed as required. The mirror system has been in use for fluorescence micro-probe measurements at 8-BM.

The authors would like to thank Kurtz Goetze from the BCDA group for helping with the software motor controls and Chris Jacobsen for his support. Scientists at beamline 10-ID (MR-CAT) at the APS provided the tungsten wire sample. Use of the Advanced Photon Source, an Office of Science User Facility operated for the US Department of Energy (DOE) Office of Science by Argonne National Laboratory, was supported by the US DOE under Contract No. DE-AC02-06CH11357.

## References

- Assoufid, L., Brown, N., Crews, D., Sullivan, J., Erdmann, M., Qian, J., Jemian, P., Yashchuk, V. V., Artemiev, N. A., Merthe, D. J., McKinney, W. R., Takacs, P. Z., Siewert, F. & Zeschke, T. (2012). *Nucl. Instrum. Methods Phys. Res. A*, **710**, 31–36.
- Assoufid, L., Qian, J., Kewish, C. M., Liu, C., Conley, R. & Macrander, A. T. (2007). *Proc. SPIE*, **6704**, 670406.
- Bilderback, D. H. (2003). *X-ray Spectrom.* **32**, 195–207.
- Ice, G. E., Budai, J. D. & Pang, J. W. L. (2011). *Science*, **334**, 1234–1239.
- Ice, G. E., Chung, J. S., Tischler, J. Z., Lunt, A. & Assoufid, L. (2000). *Rev. Sci. Instrum.* **71**, 2635.
- Kang, H. C., Maser, J., Stephenson, G. B., Liu, C., Conley, R., Macrander, A. T. & Vogt, S. (2006). *Phys. Rev. Lett.* **96**, 127401.
- Kewish, C. M., Assoufid, L. A., Macrander, A. T. & Qian, J. (2007). *Appl. Opt.* **46**, 2010–2021.
- Kirkpatrick, P. & Baez, A. V. (1948). *J. Opt. Soc. Am.* **38**, 766–774.
- Kujala, N. G., Karanfil, C. & Barrea, R. A. (2011). *Rev. Sci. Instrum.* **82**, 063106.
- Lang, J. C., Srajer, G., Wang, J. & Lee, P. L. (1999). *Rev. Sci. Instrum.* **70**, 4457.
- Larson, B. C. & Levine, L. E. (2013). *J. Appl. Cryst.* **46**, 153–164.
- Larson, B. C., Yang, W., Ice, G. E., Budai, J. D. & Tischler, J. Z. (2002). *Nature (London)*, **415**, 887–890.
- Liu, C., Conley, R., Assoufid, L., Cai, Z., Qian, J. & Macrander, A. T. (2004). *AIP Conf. Proc.* **705**, 704–707.
- Liu, C., Ice, G., Liu, W., Assoufid, L., Qian, J., Shi, B., Khachatryan, R., Wiczorek, M., Zschack, P. & Tischler, J. Z. (2012). *Appl. Surf. Sci.* **258**, 2182–2186.
- Liu, W., Ice, G. E., Assoufid, L., Liu, C., Shi, B., Khachatryan, R., Qian, J., Zschack, P., Tischler, J. Z. & Choi, J.-Y. (2011). *J. Synchrotron Rad.* **18**, 575–579.
- Liu, W. J., Ice, G. E., Tischler, J. Z., Khounsary, A., Liu, C., Assoufid, L. & Macrander, A. T. (2005). *Rev. Sci. Instrum.* **76**, 113701.
- Macrander, A. T., Kujala, N., Marathe, S., Huang, X. & Assoufid, L. (2013). *Proceedings of the 17th Pan-American Synchrotron Radiation Instrumentation Conference*. Poster presentation.
- Mimura, H., Handa, S., Kimura, T., Yumoto, H., Yamakawa, D., Yokoyama, H., Matsuyama, S., Inagaki, K., Yamamura, K.,

- Yasuhisa, S., Tamasaku, K., Nishino, Y., Yabashi, M., Ishikawa, T. & Yamauchi, K. (2010). *Nat. Phys.* **6**, 57–60.
- Montel, M. (1957). Editor. *X-ray Microscopy with Catamorphic Roof Mirrors*, in *X-ray Microscopy and Microradiography*, pp. 177–185. New York: Academic Press.
- Paunesku, T., Wanzer, M. B., Kirillova, E. N., Muksinova, K. N., Revina, V. S., Lyubchansky, E. R., Grosche, B., Birschwilks, M., Vogt, S., Finney, L. & Woloschak, G. E. (2012). *Health Phys.* **103**, 181–186.
- Qian, J., Sullivan, J., Erdmann, M., Khounsary, A. & Assoufid, L. (2012). *Nucl. Instrum. Methods Phys. Res. A*, **710**, 48–51.
- Shi, B., Liu, C., Qian, J., Liu, W., Assoufid, L., Khounsary, A., Conley, R. & Macrander, A. T. (2010). *Proc. SPIE*, **7802**, 78020G.
- Shu, D., Harder, R., Almer, J., Kujala, N., Kearney, S., Anton, J., Liu, W., Lai, B., Maser, J., Finney, L., Shi, B., Qian, J., Marathe, S., Macrander, A., Tischler, J., Vogt, S. & Assoufid, L. (2013). *Proc. SPIE*, **8836**, 88360O.
- Snigirev, A., Kohn, V., Snigireva, I. & Lengeler, B. (1996). *Nature (London)*, **384**, 49–51.
- Suzuki, Y. (2004). *Jpn. J. App. Phys.* **43**, 7311–7314.
- Weekley, C., Aitken, J., Finney, L., Vogt, S., Witting, P. & Harris, H. (2013). *Nutrients*, **5**, 1734–1756.
- Yamamura, K., Yamauchi, K., Mimura, H., Sano, Y., Saito, A., Endo, K., Souvorov, A., Yabashi, M., Tamasaku, K., Ishikawa, T. & Mori, Y. (2003). *Rev. Sci. Instrum.* **74**, 4549.
- Yasa, M., Li, Y., Mammen, C. B., Als-Nielsen, J., Hoszowska, J., Mocuta, C. & Freund, A. (2004). *Appl. Phys. Lett.* **84**, 4744.
- Yun, W., Lai, B., Cai, Z., Maser, J., Legnini, D., Gluskin, E., Chen, Z., Krasnoperova, A. A., Vladimirsky, Y., Cerrina, F., Di Fabrizio, E. & Gentili, M. (1999). *Rev. Sci. Instrum.* **70**, 2238.